HEALTH AND MEDICINE

Tracking of spaceflight-induced bone remodeling reveals a limited time frame for recovery of resorption sites in humans

Matthias Walle[1,2], Leigh Gabel[1,3,4], Danielle E. Whittier[1,4], Anna-Maria Liphardt[5,6], Paul A. Hulme[1], Martina Heer[7,8], Sara R. Zwart[9], Scott M. Smith[10], Jean D. Sibonga[10], Steven K. Boyd[1,2,11]*

Mechanical unloading causes bone loss, but it remains unclear whether disuse-induced changes to bone microstructure are permanent or can be recovered upon reloading. We examined bone loss and recovery in 17 astronauts using time-lapsed high-resolution peripheral quantitative computed tomography and biochemical markers to determine whether disuse-induced changes are permanent. During 6 months in microgravity, resorption was threefold higher than formation. Upon return to Earth, targeted bone formation occurred in high mechanical strain areas, with 31.8% of bone formed in the first 6 months after flight at sites resorbed during spaceflight, significantly higher than the 2.7% observed 6 to 12 months after return. Limited bone recovery at resorption sites after 6 months on Earth indicates a restricted window for reactivating bone remodeling factors in humans. Incomplete skeletal recovery may arise from these arrested remodeling sites, representing potential targets for new interventions, thus providing means to counteract this long-term health risk for astronauts.

INTRODUCTION

Bone is a metabolically active tissue undergoing constant modeling and remodeling to repair microdamage and adapt its structure to mechanical forces (*1*, *2*), requiring intricate coordination between bone-resorbing osteoclasts and bone-forming osteoblasts (*3*, *4*). The reversal phase serves as a critical transitional stage, mediating the coupling of these two cell types to maintain a healthy bone balance. During reversal, mononuclear cells prepare resorbed sites for new bone formation (*5*). However, in certain conditions, these sites fail to progress to formation, becoming arrested with no osteoblasts present (*6*). An accumulation of such arrested sites disrupts the delicate balance between bone resorption and formation leading to compromised bone microstructure and strength (*7*). While biopsy and histomorphometry provide insight into reversal mechanisms ex vivo (*6*–*9*), these techniques cannot track the progression of reversal sites in vivo over prolonged time frames. Consequently, the impact of persistent conditions causing bone loss on reversal sites is poorly understood. Periods of disuse or unloading, such as microgravity, injury, or immobilization, disrupt bone remodeling and cause microarchitectural decay (*10*–*12*). However, it remains unclear whether prolonged disuse leads to arrested reversal sites or complete trabecular resorption, both of which could prevent structural recovery upon reloading. Studies in astronauts have explored the effects of reexposure to Earth's gravity on bone density, microstructure and turnover post-mission, noting changes and partial recoveries (*13*–*15*), but none have fully addressed the spatiotemporal dynamics of bone formation and resorption at a local level. Understanding the timescale and potential for resorption sites to stimulate formation after disuse is critical to determine whether recovery of bone microstructure is possible or whether changes become permanent over time.

With recent computational advances in high-resolution peripheral quantitative computed tomography (HR-pQCT) imaging, we have developed methods that enable monitoring changes in bone microstructure at a resolution that allows direct identification of bone formation and resorption sites in humans (*16*). Further, this technique enables us to visualize and quantify active reversal and arrested remodeling sites in vivo, which we can leverage to delineate the roles of these specific phases in driving bone loss. Long-duration spaceflight provides a unique model for skeletal unloading due to microgravity conditions. This study establishes the spatiotemporal dynamics of skeletal remodeling (including modeling and remodeling processes) across 4- to 7-month missions and 12-month recovery on Earth for 17 astronauts. We hypothesized that resorbed areas during microgravity would provide a substrate for spatially targeted bone formation after reintroduction of mechanical loading post-flight. Our results show increased bone resorption during skeletal unloading and increased bone formation upon return to Earth, as captured by HR-pQCT imaging. These microstructural changes corresponded with fluctuations in biochemical bone turnover markers. Spatially, bone formation and resorption were associated with areas of increasing and decreasing mechanical strain, respectively, as identified through finite element analysis. Within the first 6 months after flight, a significant portion of bone formation targeted areas previously resorbed during microgravity, whereas later new areas in the bone microstructure were targeted. These results suggest a mechanically controlled and time-dependent recovery of bone resorption sites.

[1]McCaig Institute for Bone and Joint Health, University of Calgary, 3280 Hospital Drive NW, Calgary T2N 4Z6, Canada. [2]Department of Radiology, Cumming School of Medicine, University of Calgary, Calgary, Canada. [3]Human Performance Laboratory, Faculty of Kinesiology, University of Calgary, Calgary, Canada. [4]Alberta Children's Hospital Research Institute, Department of Cell Biology and Anatomy, University of Calgary, Calgary, Canada. [5]Department of Internal Medicine 3—Rheumatology & Immunology, Universitätsklinikum Erlangen & Friedrich-Alexander-Universität Erlangen-Nürnberg, Erlangen, Germany. [6]Deutsches Zentrum Immuntherapie, Universitätsklinikum Erlangen & Friedrich-Alexander-Universität Erlangen-Nürnberg, Erlangen, Germany. [7]IU International University of Applied Sciences, Health Sciences, Erfurt, Germany. [8]Department of Nutrition and Food Science, Nutritional Physiology, University of Bonn, Bonn, Germany. [9]Department of Preventive Medicine and Population Health, University of Texas Medical Branch, Galveston, TX, USA. [10]Human Health and Performance Directorate, NASA Lyndon B. Johnson Space Center, Houston, TX, USA. [11]Department of Biomedical Engineering, Schulich School of Engineering, University of Calgary, Calgary, Canada.
*Corresponding author. Email: skboyd@ucalgary.ca

RESULTS

Mechanical unloading induces bone resorption, and reloading stimulates bone formation; quantitative evidence from time-lapsed high-resolution CT imaging in vivo

We analyzed the effect of microgravity on bone resorption and formation in astronauts using HR-pQCT (XtremeCT II, Scanco Medical AG, 61 μm resolution). We scanned the distal tibiae of 17 astronauts before spaceflight and after returning to Earth (R) at R + 0 days, R + 6 months, and R + 12 months (Fig. 1 and Table 1). We calculated the total resorption (Tt.R) and formation fraction (Tt.F) between two consecutive time points as a percentage of the total bone volume, using the average values from both tibiae (Fig. 2A). In microgravity, bone resorption was three times higher on average than formation (Tt.R = 2.5 ± 2.2%, Tt.F = 0.6 ± 0.8%, $P < 0.01$).

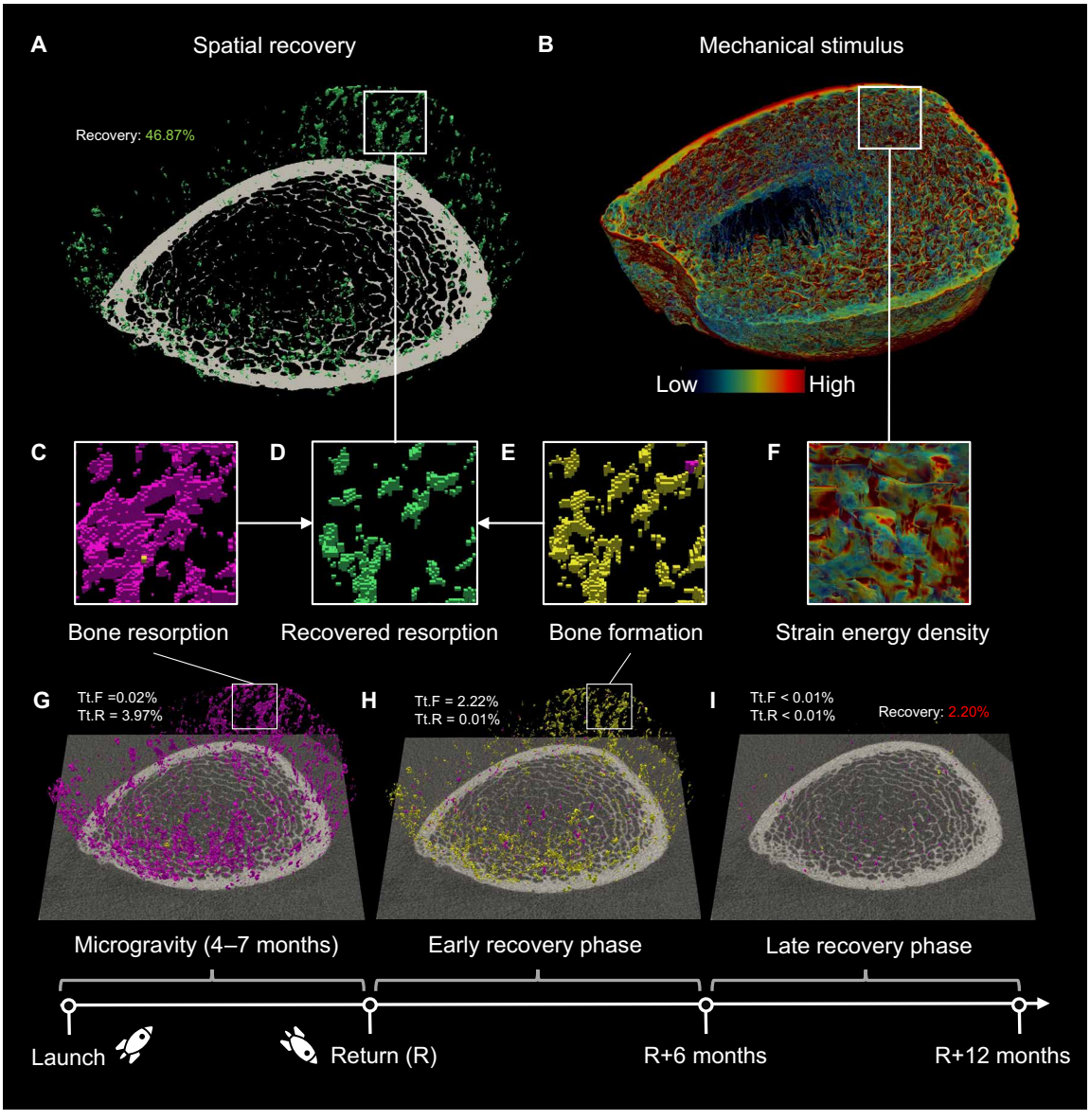

Fig. 1. Spatial recovery and mechanoregulation of bone remodeling in astronauts. We investigated whether coupling factors or mechanical signals dictate the recovery of resorption sites by bone formation in 17 astronauts during 4- to 7-month missions and 1 year recovery. The outcomes of the study are illustrated using 3D visuals of a distal tibia bone from a representative astronaut, obtained through high-resolution peripheral quantitative computed tomography. (**A**) Spatial recovery was assessed by analyzing coupled bone formation at previous resorption sites. (**B**) The mechanical stimulus at the same sites was simulated using finite element analysis to assess the mechanoregulation of bone remodeling. (**C** to **E**) Detailed views showing bone resorption sites in purple (C), recovered resorption sites in green (D), and all bone formation sites in orange (E). (**F**) Detailed view of the mechanical signal stimulus quantified by strain energy density to assess whether bone resorption and formation were more likely to occur in regions of low mechanical strain (shades of blue) and high strain (shades of red), respectively. (**G**) Our results demonstrated that bone loss due to the absence of gravitational loading was primarily driven by bone resorption. (**H**) In the first 6 months after return to Earth, increased bone formation occurred and targeted previous resorption sites. (**I**) In the following 6 months, bone formation decreased and targeted new regions in the microstructure. Throughout the recovery, we identified a relationship between remodeling sites and mechanical signals. This finding, along with identified time constraints for recovery, suggested that bone remodeling was jointly influenced by mechanical stimuli and biological coupling factors.

Table 1. Astronaut cohort characteristics. Baseline demographic and physiological data for 17 long-duration International Space Station mission participants. Values are presented as mean ± SD where applicable.

Total crew members	***n* = 17**
Sex	14 male, 3 female
Age (years)	46.9 ± 6.7
Height (cm)	177.7 ± 6.0
Body mass (kg)	79.1 ± 7.7
Body mass index (kg/m^2)	25.0 ± 2.1
Space flight duration (days)	170 ± 30
Individuals with in-flight bone turnover marker measurements	*n* = 17 (CTX-I: *n* = 14)
First-time long-duration flight participants	*n* = 14
Excluded scans due to motion artifacts	5
Medication use	None (anti-resorptive or other bone-related medication)
Supplementation	800 IU vitamin D3 daily

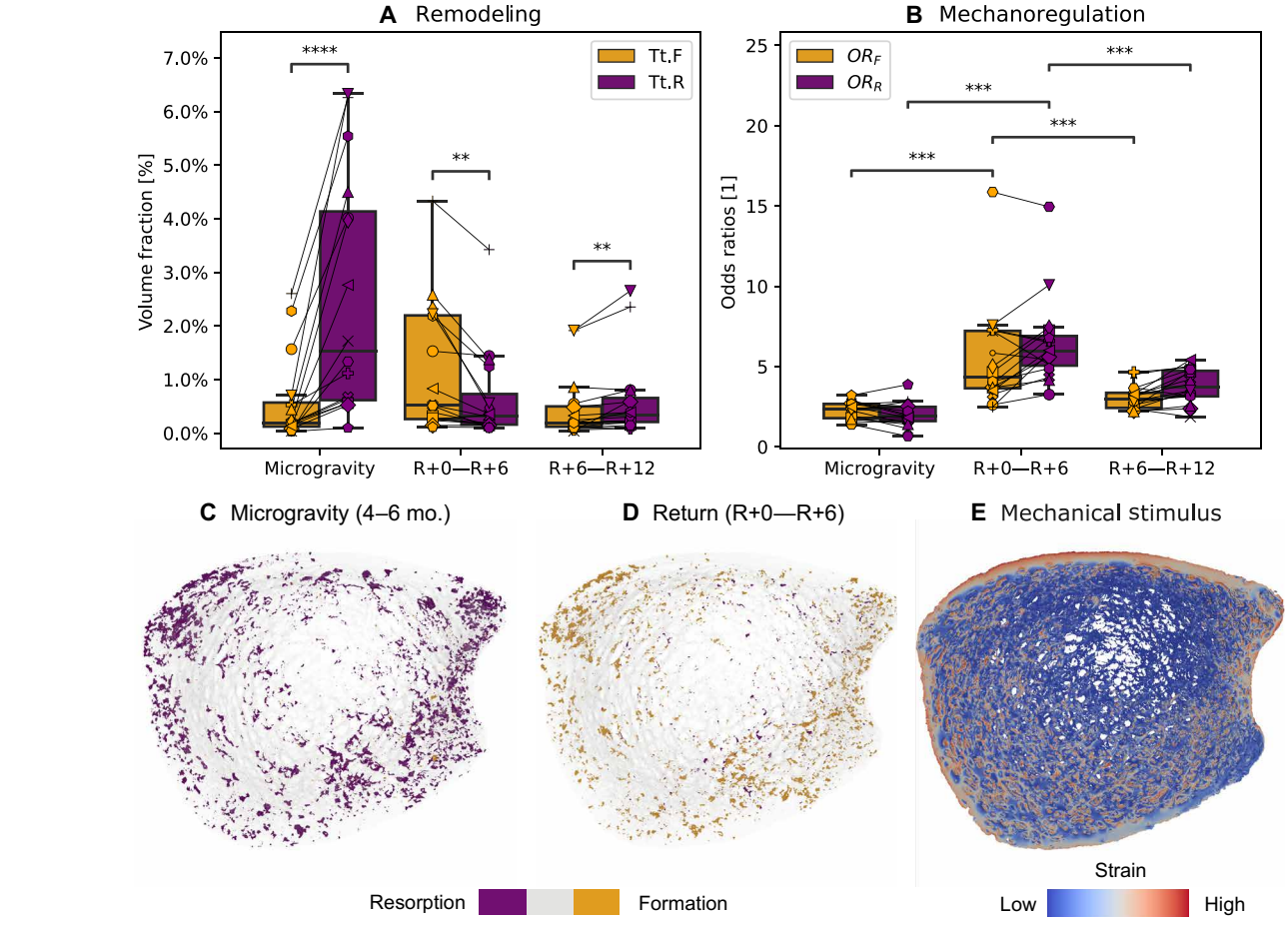

Fig. 2. Bone remodeling activity visualized in vivo by HR-pQCT at the distal tibia. (**A**) Total formation (Tt.F) and resorption (Tt.R) quantified over the mission timeline at the distal tibia reveal imbalanced turnover in microgravity that reverses within the first 6 months (R + 0 days—R + 6 months) after flight and stabilizes in the second 6 months (R + 6—R + 12 months) of recovery. Individual markers represent individual astronauts. Significant differences between Tt.F and Tt.R are indicated (**$P < 0.01$, ****$P < 0.0001$). (**B**) Participant odds ratios quantify the mechanoregulation of formation (OR_F) and resorption (OR_R) events. OR_F and OR_R reflect the percent change in formation or resorption likelihood per percent strain change. Notably, there is an increase in both OR_F and OR_R upon return to Earth, indicating adaptation to gravitational forces during reconditioning. Significant differences between time points are indicated (***$P < 0.001$). (**C** and **D**) Representative images show bone microstructure with resorption (purple) and formation (orange) sites that occurred during microgravity (C) and within the first 6 months of reloading after flight (D). (**E**) Strain distribution in bone microstructure simulated using micro–finite element (FE) analysis. Micro-FE analysis is a computational technique to estimate local deformations (i.e., strain) by simulating a virtual mechanical compression test of the bone microstructure. Color map represents strain magnitude under simulated gravitational loading.

Resorption strongly correlated with mission duration, indicating greater resorption with longer microgravity exposure ($r = 0.69$, $P < 0.01$). Upon return, participants exhibited heightened formation, exceeding resorption during the first 6 months, suggesting a limited window for recovery (Tt.F = 1.2 ± 1.2%, Tt.R = 0.7 ± 0.8%, $P < 0.01$). By 12 months, formation and resorption only showed minor differences, indicating balanced bone remodeling (Tt.F = 0.5 ± 0.6%, Tt.R = 0.6 ± 0.7%, $P < 0.01$). While individual responses varied, these findings indicate that unloading stimulates bone resorption leading to bone loss. In contrast, gravitational reloading stimulates bone formation, especially within the first 6 months of return.

Micro–finite element simulations reveal altered load-driven bone remodeling patterns during weightlessness

On Earth, weight-bearing compressive loads are an important driver of bone remodeling (*17*), but microgravity greatly reduces the mechanical forces acting on bone. To examine whether bone remodeling still follows normal Earth-bound load-driven patterns in space, we performed compressive micro–finite element analysis to simulate mechanical strains within the bone structure at each imaging time point. We spatially mapped these strains to the location of remodeling sites identified from the HR-pQCT images. We assessed the mechanoregulation of bone remodeling as the association between bone formation and resorption and local mechanical strain using logistic regression and odds ratios (Fig. 2B). These simulations revealed decreased odds of both formation and resorption ($OR_F = 2.3 \pm 0.5$, $OR_R = 2.0 \pm 0.7$) sites in the microstructure in relation to the local mechanical strains, indicating a weaker relationship with increasing/decreasing strain during microgravity compared to return ($OR_F = 5.5 \pm 3.2$, $OR_R = 6.5 \pm 2.7$). These findings suggest that in the absence of normal gravitational loading, bone remodeling follows an altered spatial pattern, likely driven by noncompressive forces experienced in microgravity (e.g., muscle forces during exercise).

Consistent bone resorption and recovery across skeletal sites support systemic metabolic responses; biochemical bone turnover markers corroborate in vivo imaging

To further characterize whether bone resorption and recovery were systemic responses or driven by regional influences, we compared measurements from the left and right tibiae with biochemical bone turnover markers in astronauts. We found a strong relationship between bone remodeling ($r = 0.87$, $P < 0.01$) and mechanoregulation measures ($r = 0.70$, $P < 0.05$) between left and right skeletal sites, indicating consistent bone resorption at different sites. To characterize the temporal progression of bone remodeling in-flight, when HR-pQCT scanning was not possible, we evaluated biochemical bone turnover markers at multiple time points during and after the missions. We found that bone remodeling (formation Tt.F and resorption Tt.R) generally correlated with corresponding bone turnover markers (formation markers P1NP and OCN and resorption markers CTX-I and NTX-I) measured over the same assessment periods (Fig. 3). The limited correlations between bone formation measurements during spaceflight (Fig. 3C) were likely due to restricted bone formation in microgravity. Furthermore, we found sclerostin, an osteocyte-secreted inhibitor of bone formation, inversely correlated with Tb.R and Tb.F on Earth, likely due to coupling between bone formation and resorption. Sclerostin also correlated with finite element method–based mechanoregulation measures OR_F ($r = 0.50$, $P < 0.05$) during recovery, further supporting our findings that bone recovery is mechanically driven, as sclerostin is involved in transducing mechanical signals in osteocytes to coordinate bone remodeling (*18*).

Long-term spatiotemporal tracking reveals a limited time frame for recovery of disuse-induced bone resorption sites

Last, we assessed whether specific regions in the bone microstructure that resorbed during spaceflight were later recovered at the same spatial locations after return to Earth. This allowed us to evaluate the spatial coupling between osteoclastic resorption and osteoblastic formation (Fig. 4). We found that 31.8 ± 9.7% of bone formed during the first 6 months of recovery (R + 0 to R + 6 months) occurred at sites previously resorbed during spaceflight, significantly more than the later phase (R + 6 to R + 12 months) with only 2.7 ± 3.0% at recovered sites. Furthermore, 6.0 ± 1.3% of bone formed during spaceflight was resorbed upon return to Earth in this early recovery phase, indicating readaptation toward preflight bone conditions. Our data indicate that there is a window for spatial recovery of disuse-induced bone resorption that is constrained to the first 6 months after reloading.

We used the difference between first and last measured bone turnover biomarkers CTX-I in-flight as a proxy for the timing of resorption during the mission. Individuals with a greater increase in CTX-I from beginning to end of the mission likely experienced more bone resorption occurring later in flight compared to those with smaller or no CTX-I increases over the mission duration. To determine whether the timing of flight resorption affects bone recovery, we assessed correlations between in-flight CTX-I increase (ΔCTX-I) and the fraction of spatially recovered resorption sites during early recovery. ΔCTX-I positively and significantly correlated with the fraction of spatially recovered resorption sites ($r = 0.63$, $P < 0.05$). These results suggest that the extent of spatial recovery of resorbed bone microstructure after flight depends on the duration between resorption events and subsequent reloading on Earth.

DISCUSSION

The results of this study provide insights into the spatiotemporal dynamics of bone remodeling during long-duration spaceflight and post-flight recovery. In our previous research, we observed significant bone resorption at weight-bearing sites such as the distal tibia during 4 to 7 months in microgravity (*13*). Our data provide insight by tracking localized three-dimensional bone resorption and formation sites during microgravity exposure and extended postflight time frame in addition to connecting remodeling events with mechanical stimuli at the tissue level. This approach sheds light on the relationship between localized bone resorption, reversal transition sites, and mechanically induced bone remodeling. It shows where resorption-driven bone loss occurs during unloading and how there is limited viability to recover disuse-induced resorption after reloading on Earth.

The time-lapsed HR-pQCT analysis revealed how mechanical unloading induces sites of bone resorption and the patterns of bone formation stimulated during reloading at the distal tibia. Our results provide mechanistic insight into previous research showing significant density losses after spaceflights, predominantly at the weight-bearing skeleton (*19*). We demonstrate that the normal association between local mechanical loads and bone turnover is disrupted when these forces are removed in microgravity, leading to elevated bone

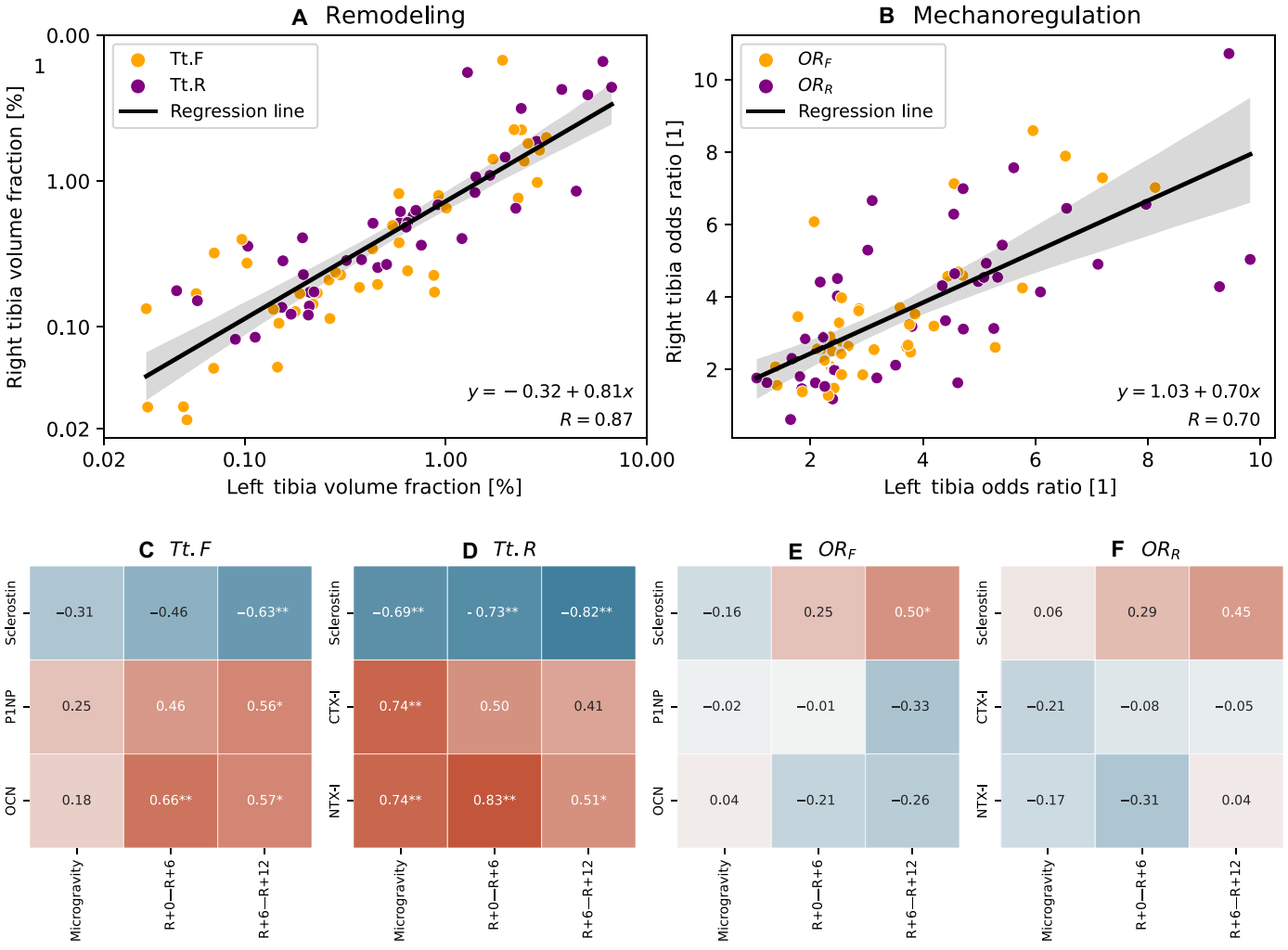

Fig. 3. Connecting local and systemic bone turnover. (**A** and **B**) Correlations between remodeling measures (Tt.F, Tt.R) represented on log scale (A) and mechanoregulation (OR_F, OR_R) of the left and right distal tibia (B). (**C** to **F**) Correlations between these metrics and absolute bone turnover markers, including osteocalcin (OCN), procollagen 1 N-terminal propeptide (P1NP), sclerostin, C-telopeptide of cross-linked collagen type I (CTX-I), and type I collagen N-telopeptide (NTX-I). Correlations performed using Spearman's rank correlation, where positive associations are shaded in red, and negative correlations are in blue. This analysis assesses relationships between local bone remodeling outcomes from high-resolution peripheral quantitative computed tomography and systemic bone metabolic activity. Biochemical bone turnover markers were measured in serum and urine during the following periods: in-flight (FD15-FD180), 6 months post-flight (R + 1, R + 6) and 12-months post-flight (R + 12). Original data on bone turnover markers are available in a previously published work (*13*). Significant correlations are indicated (*$P < 0.05$, **$P < 0.01$).

resorption and subsequent bone loss. While histological and biochemical findings from animal models often suggest that unloading leads to an altered remodeling balance dominated by reduced formation (*20*–*23*), human studies have indicated increased biochemical markers for bone resorption (*24*–*27*) with little effect on bone formation markers (*25*, *28*). Direct comparisons are challenging due to limitations in both approaches: Animal models are influenced by factors like strain and age, while biochemical measures struggle to distinguish localized responses (*19*). While resistive exercise has been shown to increase bone formation markers (*29*), uncertainty remains regarding the relative contribution of reduced bone formation during weightlessness at these sites (*10*–*12*). By directly measuring the volume of formed and resorbed bone, our results provide quantitative evidence that supports the notion that primarily elevated resorption dominates bone loss during unloading. Notably, using noninvasive methods, we demonstrate this spaceflight-associated increase in bone resorption directly in human tissue, consistent with findings from invasive histomorphometry and iliac crest biopsies in human bed rest studies (*30*, *31*).

The mechanoregulation analysis indicated a notable reduction in the correlation between micro–finite element–simulated localized bone strains and observed microgravity-induced bone remodeling activity compared to postflight measurements. This finding signifies that the strains induced by gravity no longer reflect the predominant mechanical forces driving bone adaptation in non–weight-bearing conditions during spaceflight. Instead, alternative stimuli regulate remodeling activity in microgravity, for example, tibial muscle forces that differ from purely compressive loading (*32*). Osteocyte-associated sclerostin continued regulating bone formation and resorption in space but decoupled from our simulated mechanoregulation

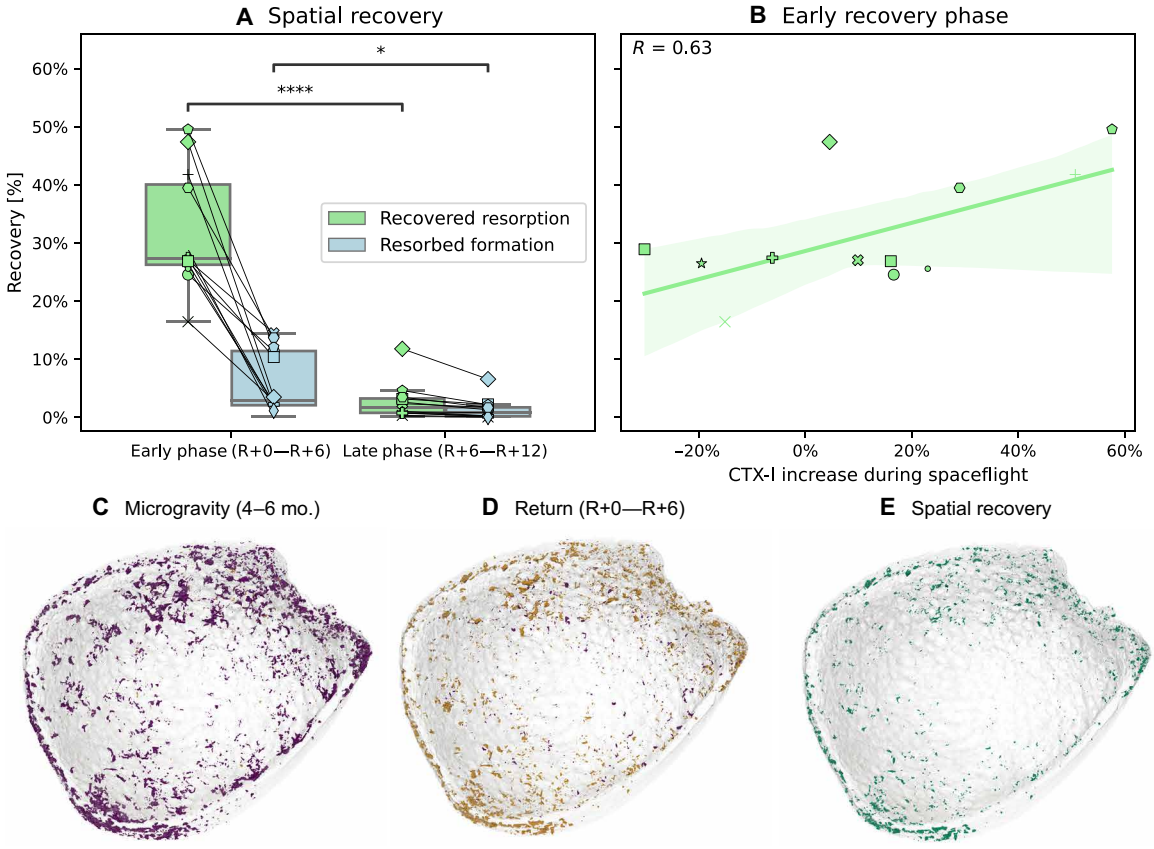

Fig. 4. Bone recovery after spaceflight. (**A**) Recovery of resorbed bone during early (R + 0 to R + 6 months) and late (R + 6 to R + 12 months) phases at the exact spatial locations previously resorbed in microgravity. Also shown is subsequent resorption after return to Earth at sites formed in microgravity. Individual markers represent individual astronauts. Significant differences between time points are indicated (*$P < 0.05$, ****$P < 0.0001$). (**B**) Linear regression between recovered resorption (early phase) and increase in CTX-I during spaceflight (measured on flight day 15 and before return on flight day 120 or 180). (**C** and **D**) Representative high-resolution peripheral quantitative computed tomography images show bone microstructure with resorption (purple) and formation (orange) sites identified in (C) microgravity and (D) at 6 months after return to Earth. (**E**) Spatial recovery of the same locations previously resorbed in microgravity during the early recovery phase. Periosteal contraction representing reduced cross-sectional area (i.e., bone size) during spaceflight and subsequent expansion may drive the observed elevated periosteal remodeling, potentially explaining previously reported post-mission changes in bone size (*15*).

markers, further supporting the role of alternative stimuli. Over time, prolonged mismatches in tissue loading between microgravity and gravitational environments may alter microstructural alignment, even if bone mineral density appears stable initially. This space-adapted microstructure becomes mismatched with Earth's gravitational demands upon return, necessitating a readaptation process. This would explain why some bone formed during the mission is subsequently resorbed on Earth and align with studies reporting resorption after return to Earth in some individuals, such as the postflight losses observed in cosmonauts after a 6-month sojourn in the International Space Station (ISS) at the distal radius (*14*). Our results support the necessity of monitoring both bone density, strength, and microarchitectural changes to fully evaluate mechanically induced bone deficits and strength recovery after long durations of mechanical unloading. Further, assessing bone mechanoregulation could help identify individuals at risk for bone loss upon return, or aid in the identification of underloaded areas to guide optimized exercise countermeasures in-flight, such as incorporating multi-loading exercises that include bending and torques in addition to tension and compression.

The tracking of bone remodeling sites in microgravity and after return to Earth revealed that the first 6 months after return to Earth represent a crucial period for successful recovery, indicating potential "expiry dates" for recovery of disuse-induced bone resorption sites. Not only did most of the bone formation take place then, but notably, a large fraction of the bone formed in that time frame was in the exact anatomical locations where bone had been lost during unloading. It is important to note that while our analysis aimed to capture this intricate process, the inherent limitations of HR-pQCT time-lapse imaging and potential artifacts near the signal-to-noise threshold make it challenging to detect all coupled remodeling events with complete certainty (*16*). Specifically, some bone formation may have occurred in areas where bone resorption occurred before our initial scan. Further, some resorption sites may have fully removed the underlying trabecular structures, necessitating new bone formation at alternate locations to maintain mechanical integrity because previous structures cannot be recreated. Overall, our findings suggest that the time since resorption seems to affect whether local bone formation occurs at the same sites. Recent ex vivo research has identified active and arrested reversal surfaces, where arrested surfaces signify a stalled or aborted reversal phase that does not transition to bone formation (*6*–*8*). The limited spatial recovery observed in the later phase, compared to the observed

reversibility and spatial coupling during the first 6 months, indicates that prolonged elevation of resorption and prolonged absence of subsequent formation may turn older resorption sites into arrested sites, or completely remove trabecular structures, that cannot be efficiently recovered upon return. Whether this site-specific formation is driven by growth factors released from the resorbed bone matrix, localized mechanical strain, or a combination of both remains unclear and warrants further investigation.

Our study has some limitations. While our previous precision study showed no significant difference in short-term and 1-year precision between formation and resorption detection (*16*), it is important to note that the slower mineralization process of bone formation may lead to ongoing events not captured within this time frame. In addition, while our precision analysis was conducted at the tissue level, the detection of local volumes may present further challenges. Future studies should further validate this technique using histomorphometry to verify agreement of bone formation sites measured with HR-pQCT. Follow-up beyond 1 year would help confirm longer-term bone recovery patterns after spaceflight. Further, more frequent testing within the first year after flight could help identify more precise time limits for the proposed bone recovery timeline. We assessed bone remodeling and mechanoregulation at the distal tibiae, which included both the left and right sides. However, it is well established that the skeletal effects of mechanical loading are locally induced, which may limit the generalizability of our findings to other skeletal sites, particularly non–weight-bearing ones. Moreover, at skeletal sites primarily composed of cortical bone, the higher prevalence of inherently uncoupled cortical bone modeling through periosteal expansion may obscure the detection of coupled remodeling events (*15*). We chose the distal tibia because other common sites like the distal radius are less affected by microgravity exposure (*33*) and have more motion artifacts that require the exclusion of data. Focusing on gravitational loading in the distal tibia rather than incorporating other mechanical influences like muscle forces (*34*) enabled a clearer examination of bone changes resulting specifically from reduced gravitational tissue loading. Strengths include bilateral assessment providing corroborating data supporting systematic changes, multiple longitudinal scans enabling quantification of turnover at several time points, and stringent quality control of HR-pQCT imaging. Last, increasing female representation in spaceflight missions will enable future studies to better evaluate potential sex differences in responses to microgravity.

In summary, this study provides insights into skeletal dynamics during prolonged mechanical unloading in spaceflight and postflight recovery in a sizable cohort of astronauts over a considerable length of time. Using advanced three-dimensional (3D) imaging combined with biochemical markers, we characterized patterns of local resorption and formation during weightlessness and upon return to Earth. Our data, based on observations of the microstructure directly, showed up-regulated bone resorption activity as the primary driver of spaceflight-induced bone loss rather than suppressed bone formation. From this, we postulate that the increased resorption observed in microgravity may result from a disrupted reversal phase, leading to more prolonged resorption phases. In the absence of bone formation, resorption sites may turn into arrested sites that are not recoverable if abandoned for too long. Our results indicate a strong relationship between recovery sites and mechanics; therefore, we propose that mechanics and coupling factors work together to control this process and establish time limits for viable recovery. Despite the mechanical stimulation during the second 6 months after return, unloading-induced resorption sites may have become arrested, rendering the process ineffective. This research not only has important implications for long-duration spaceflight but more broadly contributes to understanding fundamental mechanisms of bone adaptation to mechanical loads, applicable beyond microgravity.

MATERIALS AND METHODS

This prospective study included 17 astronauts from the National Aeronautics and Space Administration (NASA), Canadian Space Agency, European Space Agency (ESA), and Japan Aerospace Exploration Agency (JAXA) who were selected for missions to the ISS (*13*, *35*). This study was approved by the University of Calgary Conjoint Health Research Ethics Board (REB14-0573), NASA Institutional Review Board (NASA7116301606HR), ESA Human Research Multilateral Review Board (TBone Pro 1261), and JAXA Institutional Review Board for Human Research (JX-IRBA-20-027). All participants provided written informed consent. Astronauts were provided 800 IU of vitamin D3 supplements daily during spaceflight and followed a carefully planned near-daily exercise routine in space to stay healthy. This included regular aerobic exercises like treadmill running, stationary cycling, and use of the advanced resistive exercise device (ARED) that provides loads up to 272 kg allowing for barbell and cable exercises, such as squats, deadlifts, and heel raises. Their exercise routines were monitored tracking frequency, duration, and type of activities performed (*13*, *35*). After returning to Earth, astronauts underwent a reconditioning program supervised by specialists to help their bodies recover.

Image acquisition

We used high-resolution peripheral quantitative computed tomography (HR-pQCT, XtremeCT II; Scanco Medical) to assess bone microstructure and strength at the left and right distal tibiae before and after spaceflight upon return to Earth (R) at R + 0 days, R + 6 months, and R + 12 months. HR-pQCT scans were performed according to standard in vivo protocols (*36*), acquiring a 10.2-mm scan region beginning 22.5 mm proximal to the distal tibia endplate. Follow-up scans were aligned as closely as possible to preflight positioning. Each scan consists of 168 slices at 60.7 μm nominal isotropic resolution, per the manufacturer's standard clinical protocol. Cortical and trabecular contours were automatically identified using a dual-threshold technique (*37*) (cortical bone: 450 mg HA/cm^3, trabecular bone: 320 mg HA/cm^3) and manually corrected if needed (*38*). Scans were automatically graded for motion artifacts that can occur during scanning on a five-point scale (1 is least motion and 5 is greatest motion) and manually verified (*39*). To reduce noise, left and right tibia measurements from scans with motion scores ≤ 2 were averaged for analysis. For participants who had scans with motion scores > 2 ($n = 7$), only scans without motion artifacts were used for further analysis (*16*).

Biochemical assessment

Biochemical data were obtained through data sharing with NASA's Biochemical Profile and Spaceflight Standard Measures studies. Fasting urine and blood samples were collected on flight days 15, 30, 60, 120, and 180 (FD15-FD180) during spaceflight and upon return to Earth (R + 0), 1 month (R + 1), 6 months (R + 6), and 12 months (R + 12) after flight. In-flight urine was limited to one 24-hour pool

per time point per crew. Assays were performed as described previously by NASA's Nutritional Biochemistry Lab (*13*, *35*). Analyzed biomarkers included urine procollagen 1 N-telopeptide [NTX-I, coefficient of variation (CV) 9.6%] and C-telopeptide of cross-linked collagen type I (CTX-I, CV 6.9%), and serum osteocalcin (OCN, CV 5.9%), sclerostin (CV 3.7%), and procollagen 1 N-terminal propeptide (P1NP, CV 4.1%). Biomarkers were averaged over HR-pQCT assessment periods during spaceflight (FD15 to FD180), early postflight (R + 0 and R + 1), and late postflight (R + 6 and R + 12). Maximum sample size was $n = 17$, except $n = 14$ for CTX-I as three astronauts did not consent to its analysis. Increases in CTX-I during spaceflight were assessed as the percent difference between first (FD15) and last available measurements (FD120 and FD180) in flight. CTX-I was selected for its more consistent inter-assay CV in this analysis.

Bone formation, resorption, and recovery sites

Bone formation and resorption sites were identified using a previously validated registration-based approach (*16*, *40*). Briefly, images were aligned by optimizing Euler angles to maximize the voxel-wise correlation of grayscale densities within the periosteal contour using a Powell algorithm and a five-level pyramid registration framework. Grayscale images were interpolated linearly and filtered to reduce noise. Binary bone segmentations and compartment masks were interpolated in a nearest-neighbor manner. The common total bone region across rescans was determined to exclude voxels outside this area. Aligned bone segmentations were superimposed to identify regions of formation and resorption. To reduce false events, identified sites were filtered to require a minimum density increase of 225 mg HA/cm^3 and a minimum cluster size of 12 voxels (*16*). Formation and resorption volumes were expressed relative to baseline mineralized bone volume. Bone recovery was assessed by quantifying the fraction of bone formation sites during the recovery phase that occurred at locations previously resorbed during spaceflight. Analogously, resorbed bone formation assessed the fraction of bone resorption sites during recovery that occurred in regions previously formed during spaceflight.

Bone mechanoregulation

Bone mechanoregulation was assessed using a previously validated method (*16*). Briefly, tissue loading was estimated as gravitational (axial) loading at the distal tibia using micro–finite element analysis. To generate the micro–finite element meshes, voxels of the segmented bone structure were converted to 8-node hexahedral elements, assigning a Young's modulus of 8.748 GPa and a Poisson's ratio of 0.3 (*41*). Compressive loading up to 1% apparent strain was calculated and solved using FAIM (version 9.0, Numerics88 Solutions Ltd., Canada) (*42*) on the University of Calgary's Advanced Research Computing cluster. Logistic regression analysis was used to assess the voxel-wise association between the mechanical signal [baseline strain energy density (SED)] and formation/resorption events to determine participant-specific, strain-driven bone remodeling. Resulting odds ratios per percentage change in normalized SED (SED/SED_{max}) for resorption (OR_R) and formation (OR_F) were used to quantify individual strain-driven remodeling.

Statistical analysis

Normally distributed variables are reported as mean and SD, while nonnormally distributed variables are presented as median and interquartile range. Student's *t* test was used to compare normally distributed variables, while the Wilcoxon–Mann–Whitney test was used to compare nonnormally distributed variables. Correlations between biochemical bone turnover markers, bone remodeling fractions, and mechanoregulation were determined by Spearman's rank correlation coefficient. A *P* value less than 0.05 was considered statistically significant for these analyses, with two-tailed testing. To adjust for multiple comparisons and minimize type I errors, Bonferroni correction was applied. All statistical analyses were performed using Python (v3.8.5).

REFERENCES AND NOTES

1. H. M. Frost, The mechanostat: A proposed pathogenic mechanism of osteoporoses and the bone mass effects of mechanical and nonmechanical agents. *Bone Miner.* **2**, 73–85 (1987).
2. H. M. Frost, Bone's mechanostat: A 2003 update. *Anat. Rec. A Discov. Mol. Cell. Evol. Biol.* **275**, 1081–1101 (2003).
3. M. B. Schaffler, W. Y. Cheung, R. Majeska, O. Kennedy, Osteocytes: Master orchestrators of bone. *Calcif. Tissue Int.* **94**, 5–24 (2014).
4. L. Qin, W. Liu, H. Cao, G. Xiao, Molecular mechanosensors in osteocytes. *Bone Res.* **8**, 23 (2020).
5. V. Everts, J. M. Delaissé, W. Korper, D. C. Jansen, W. Tigchelaar-Gutter, P. Saftig, W. Beertsen, The bone lining cell: Its role in cleaning Howship's lacunae and initiating bone formation. *J. Bone Miner. Res.* **17**, 77–90 (2002).
6. T. L. Andersen, M. E. Abdelgawad, H. B. Kristensen, E. M. Hauge, L. Rolighed, J. Bollerslev, P. Kjærsgaard-Andersen, J. M. Delaisse, Understanding coupling between bone resorption and formation: Are reversal cells the missing link? *Am. J. Pathol.* **183**, 235–246 (2013).
7. T. L. Andersen, E. M. Hauge, L. Rolighed, J. Bollerslev, P. Kjærsgaard-Andersen, J. M. Delaisse, Correlation between absence of bone remodeling compartment canopies, reversal phase arrest, and deficient bone formation in post-menopausal osteoporosis. *Am. J. Pathol.* **184**, 1142–1151 (2014).
8. C. M. Andreasen, M. Ding, S. Overgaard, P. Bollen, T. L. Andersen, A reversal phase arrest uncoupling the bone formation and resorption contributes to the bone loss in glucocorticoid treated ovariectomised aged sheep. *Bone* **75**, 32–39 (2015).
9. N. E. Lassen, T. L. Andersen, G. G. Pløen, K. Søe, E. M. Hauge, S. Harving, G. E. T. Eschen, J. M. Delaisse, Coupling of bone resorption and formation in real time: New knowledge gained from human Haversian BMUs. *J. Bone Miner. Res.* **32**, 1395–1405 (2017).
10. P. Zhang, K. Hamamura, H. Yokota, A brief review of bone adaptation to unloading. *Genomics Proteomics Bioinformatics* **6**, 4–7 (2008).
11. L. Vico, A. Hargens, Skeletal changes during and after spaceflight. *Nat. Rev. Rheumatol.* **14**, 229–245 (2018).
12. D. D. Bikle, B. P. Halloran, The response of bone to unloading. *J. Bone Miner. Metab.* **17**, 233–244 (1999).
13. L. Gabel, A. M. Liphardt, P. A. Hulme, M. Heer, S. R. Zwart, J. D. Sibonga, S. M. Smith, S. K. Boyd, Incomplete recovery of bone strength and trabecular microarchitecture at the distal tibia 1 year after return from long duration spaceflight. *Sci. Rep.* **12**, 9446 (2022).
14. L. Vico, B. van Rietbergen, N. Vilayphiou, M. T. Linossier, H. Locrelle, M. Normand, M. Zouch, M. Gerbaix, N. Bonnet, V. Novikov, T. Thomas, G. Vassilieva, Cortical and trabecular bone microstructure did not recover at weight-bearing skeletal sites and progressively deteriorated at non-weight-bearing sites during the year following International Space Station missions. *J. Bone Miner. Res.* **32**, 2010–2021 (2017).
15. T. F. Lang, A. D. Leblanc, H. J. Evans, Y. Lu, Adaptation of the proximal femur to skeletal reloading after long-duration spaceflight. *J. Bone Miner. Res.* **21**, 1224–1230 (2006).
16. M. Walle, D. E. Whittier, D. Schenk, P. R. Atkins, M. Blauth, P. Zysset, K. Lippuner, R. Müller, C. J. Collins, Precision of bone mechanoregulation assessment in humans using longitudinal high-resolution peripheral quantitative computed tomography in vivo. *Bone* **172**, 116780 (2023).
17. S. Sasimontonkul, B. K. Bay, M. J. Pavol, Bone contact forces on the distal tibia during the stance phase of running. *J. Biomech.* **40**, 3503–3509 (2007).
18. G. L. Galea, L. E. Lanyon, J. S. Price, Sclerostin's role in bone's adaptive response to mechanical loading. *Bone* **96**, 38–44 (2017).
19. M. Stavnichuk, N. Mikolajewicz, T. Corlett, M. Morris, S. V. Komarova, A systematic review and meta-analysis of bone loss in space travelers. *npj Microgravity* **6**, 13 (2020).
20. D. Amblard, M. H. Lafage-Proust, A. Laib, T. Thomas, P. Rüegsegger, C. Alexandre, L. Vico, Tail suspension induces bone loss in skeletally mature mice in the C57BL/6J strain but not in the C3H/HeJ strain. *J. Bone Miner. Res.* **18**, 561–569 (2003).
21. E. Zerath, X. Holy, S. G. Roberts, C. Andre, S. Renault, M. Hott, P. J. Marie, Spaceflight inhibits bone formation independent of corticosteroid status in growing rats. *J. Bone Miner. Res.* **15**, 1310–1320 (2000).

22. T. J. Wronski, E. R. Morey-Holton, S. B. Doty, A. C. Maese, C. C. Walsh, Histomorphometric analysis of rat skeleton following spaceflight. *Am. J. Physiol.* **252**, R252–R255 (1987).
23. J. M. Cavolina, G. L. Evans, S. A. Harris, M. Zhang, K. C. Westerlind, R. T. Turner, The effects of orbital spaceflight on bone histomorphometry and messenger ribonucleic acid levels for bone matrix proteins and skeletal signaling peptides in ovariectomized growing rats. *Endocrinology* **138**, 1567–1576 (1997).
24. A. Caillot-Augusseau, L. Vico, M. Heer, D. Voroviev, J. C. Souberbielle, A. Zitterman, C. Alexandre, M. H. Lafage-Proust, Space flight is associated with rapid decreases of undercarboxylated osteocalcin and increases of markers of bone resorption without changes in their circadian variation: Observations in two cosmonauts. *Clin. Chem.* **46**, 1136–1143 (2000).
25. S. M. Smith, M. E. Wastney, K. O. O'Brien, B. V. Morukov, I. M. Larina, S. A. Abrams, J. E. Davis-Street, V. Oganov, L. C. Shackelford, Bone markers, calcium metabolism, and calcium kinetics during extended-duration space flight on the mir space station. *J. Bone Miner. Res.* **20**, 208–218 (2005).
26. A. Caillot-Augusseau, M. H. Lafage-Proust, C. Soler, J. Pernod, F. Dubois, C. Alexandre, Bone formation and resorption biological markers in cosmonauts during and after a 180-day space flight (Euromir 95). *Clin. Chem.* **44**, 578–585 (1998).
27. S. M. Smith, S. R. Zwart, G. Block, B. L. Rice, J. E. Davis-Street, The nutritional status of astronauts is altered after long-term space flight aboard the International Space Station. *J. Nutr.* **135**, 437–443 (2005).
28. S. M. Smith, M. E. Wastney, B. V. Morukov, I. M. Larina, L. E. Nyquist, S. A. Abrams, E. N. Taran, C. Y. Shih, J. L. Nillen, J. E. Davis-Street, B. L. Rice, H. W. Lane, Calcium metabolism before, during, and after a 3-mo spaceflight: Kinetic and biochemical changes. *Am. J. Physiol. Regul. Integr. Comp. Physiol.* **277**, R1–R10 (1999).
29. S. M. Smith, M. A. Heer, L. C. Shackelford, J. D. Sibonga, L. Ploutz-Snyder, S. R. Zwart, Benefits for bone from resistance exercise and nutrition in long-duration spaceflight: Evidence from biochemistry and densitometry. *J. Bone Miner. Res.* **27**, 1896–1906 (2012).
30. J. E. Zerwekh, L. A. Ruml, F. Gottschalk, C. Y. C. Pak, The effects of twelve weeks of bed rest on bone histology, biochemical markers of bone turnover, and calcium homeostasis in eleven normal subjects. *J. Bone Miner. Res.* **13**, 1594–1601 (1998).
31. L. Vico, D. Chappard, C. Alexandre, S. Palle, P. Minaire, G. Riffat, B. Morukov, S. Rakhmanov, Effects of a 120 day period of bed-rest on bone mass and bone cell activities in man: Attempts at countermeasure. *Bone Miner.* **2**, 383–394 (1987).
32. H. Fujiya, P. Kousa, B. C. Fleming, D. L. Churchill, B. D. Beynnon, Effect of muscle loads and torque applied to the tibia on the strain behavior of the anterior cruciate ligament: An in vitro investigation. *Clin. Biomech.* **26**, 1005 (2011).
33. A. LeBlanc, V. Schneider, L. Shackelford, S. West, V. Oganov, A. Bakulin, L. Voronin, Bone mineral and lean tissue loss after long duration space flight. *J. Musculoskelet. Neuronal Interact.* **1**, 157–160 (2000).
34. M. Walle, F. C. Marques, N. Ohs, M. Blauth, R. Müller, C. J. Collins, Bone mechanoregulation allows subject-specific load estimation based on time-lapsed micro-CT and HR-pQCT in vivo. *Front. Bioeng. Biotechnol.* **9**, 486 (2021).
35. L. Gabel, A.-M. Liphardt, P. A. Hulme, M. Heer, S. R. Zwart, J. D. Sibonga, S. M. Smith, S. K. Boyd, Pre-flight exercise and bone metabolism predict unloading-induced bone loss due to spaceflight. *Br. J. Sports Med.* **56**, 196–203 (2022).
36. M. L. Bouxsein, S. K. Boyd, B. A. Christiansen, R. E. Guldberg, K. J. Jepsen, R. Müller, Guidelines for assessment of bone microstructure in rodents using micro–computed tomography. *J. Bone Miner. Res.* **25**, 1468–1486 (2010).
37. H. R. Buie, G. M. Campbell, R. J. Klinck, J. A. MacNeil, S. K. Boyd, Automatic segmentation of cortical and trabecular compartments based on a dual threshold technique for in vivo micro-CT bone analysis. *Bone* **41**, 505–515 (2007).
38. D. E. Whittier, A. N. Mudryk, I. D. Vandergaag, L. A. Burt, S. K. Boyd, Optimizing HR-pQCT workflow: A comparison of bias and precision error for quantitative bone analysis. *Osteoporos. Int.* **31**, 567–576 (2020).
39. M. Walle, D. Eggemann, P. R. Atkins, J. J. Kendall, K. Stock, R. Müller, C. J. Collins, Motion grading of high-resolution quantitative computed tomography supported by deep convolutional neural networks. *Bone* **166**, 116607 (2023).
40. D. E. Whittier, M. Walle, D. Schenk, P. R. Atkins, C. J. Collins, P. Zysset, K. Lippuner, R. Müller, A multi-stack registration technique to improve measurement accuracy and precision across longitudinal HR-pQCT scans. *Bone* **176**, 116893 (2023).
41. D. E. Whittier, S. L. Manske, D. P. Kiel, M. Bouxsein, S. K. Boyd, Harmonizing finite element modelling for non-invasive strength estimation by high-resolution peripheral quantitative computed tomography. *J. Biomech.* **80**, 63–71 (2018).
42. J. A. MacNeil, S. K. Boyd, Bone strength at the distal radius can be estimated from high-resolution peripheral quantitative computed tomography and the finite element method. *Bone* **42**, 1203–1213 (2008).

Acknowledgments: We would like to thank the astronauts for their time participating in this study; A. Cooke, S. Kwong, D. Raymond, and G. Yardley for scan acquisition and data collection; and K. Koger for study coordination. We thank the NASA Nutritional Biochemistry Lab for support of the biosample collections and biomarker analyses, the VieCuri Medical Centre (J. P. van den Bergh), and the Canadian Space Agency for strong operational support. **Funding:** This study was supported by the Canadian Space Agency (contract no. 9F053-120605—Concept Definition and no. 9F008-140715—Operational Support, PI: S.K.B.). M.W. and L.G. were supported by Alberta Innovates Health Solutions Postgraduate Fellowships. The biomarker data were shared from the Biochemistry Profile project, which was funded by the NASA Human Research Program's Human Health Countermeasures Element. The funders of the study had no role in data collection, analysis, interpretation, or writing of the report. The corresponding author had full access to all the data in the study and accepts responsibility for the decision to submit for publication. **Author contributions:** Conceptualization: A.-M.L., M.H., S.R.Z., S.M.S., J.D.S., and S.K.B. Methodology: M.W., D.E.W., S.M.S., and S.K.B. Software: M.W. and L.G. Validation: M.W., L.G., D.E.W., and S.K.B. Formal analysis: M.W. and S.K.B. Investigation: S.K.B., A.-M.L., P.A.H., M.H., S.R.Z., S.M.S., and J.D.S. Resources: S.M.S., S.K.B., and A.-M.L. Data curation: M.W., L.G., and S.K.B. Writing—original draft: M.W. and S.K.B. Writing—review and editing: M.W., L.G., D.E.W., A.-M.L., P.A.H., M.H., S.R.Z., S.M.S., J.D.S., and S.K.B. Visualization: M.W. Supervision: S.K.B. Project administration: S.K.B. Funding acquisition: S.K.B. and A.-M.L. Approval of final manuscript: All authors. **Competing interests:** The authors declare that they have no competing interests. **Data and materials availability:** All data needed to evaluate the conclusions in the paper are present in the paper and/or the Supplementary Materials. Additional data related to the manuscript are available through NASA's Lifetime Surveillance of Astronaut Health project. The NASA Life Sciences Data Archive (LSDA) is the repository for all human and animal research data, including that associated with this study. LSDA has a public facing portal where data requests can be initiated (https://lsda.jsc.nasa.gov/Request/dataRequestFAQ).

Submitted 9 May 2024
Accepted 15 November 2024
Published 20 December 2024
10.1126/sciadv.adq3632